

LONG-LIVED AUTOIONIZING STATES OF NOBLE-GAS ATOMS AND IONS

S. E. KUPRIYANOV and A. A. PEROV

I. Ya. Karpov Physico-chemical Institute

Submitted November 26, 1968

Zh. Eksp. Teor. Fiz. 56, 1524-1532 (May, 1969).

Long-lived autoionizing states of argon, krypton, and xenon atoms, and of singly-charged argon ions, are observed by the mass-spectrometric method. Special ion sources were used in which atoms were excited or ionized by electron impact, and the autoionization process was registered by means of the ions produced in a separate chamber. The long-lived autoionizing states of the atoms lie between the first and second ionization limits, $np^5 \ ^2P_{3/2}^0$ and $np^5 \ ^2P_{1/2}^0$. The low ionization rate ($\sim 10^6 \text{ sec}^{-1}$) is due to the large values of the principal quantum number n and of the orbital angular momentum of the excited electron. These states are not observed in optical spectra because of the selection rules for dipole transitions.

It is well-known that ions^[1-3] and atoms^[4,5] of the noble gases possess long-lived Rydberg states that lie near the ionization limits and that can easily undergo ionization near a metal surface in an electric field^[6] or in collisions with molecules.^[7]

The atoms and ions of the noble gases, except helium, possess two or more ionization limits to which different Rydberg series converge.¹⁾ Excited states lying above the lowest ionization limit can autoionize. Photoabsorption experiments have indicated that some of these states have short lifetimes $\sim 10^{-13}$ sec with respect to autoionization.^[8] In these experiments only optically allowed states were excited, to which dipole transitions are allowed by the selection rules; these were ns and nd states. However, electron impacts also excite optically forbidden states such as np and nf , which can possess small probabilities of autoionization. It has been reported in^[9,10] that collisions between electrons and noble-gas atoms produce long-lived autoionizing states of Ar^+ and Xe^+ ions having lifetimes $\sim 10^{-6}$ sec, but the nature of these states was not discussed. The given conclusion was based on the observed way in which the ion intensity was influenced by the initial gas pressure and electron energy.

The principal experimental results obtained in^[9,10] are that 1) in the process



the intensity of the produced doubly-charged ions A^{2+} is directly proportional to the intensity of the initial singly-charged ions A^+ , and 2) the doubly-charged ions A^{2+} are formed from the singly-charged ions in accordance with (1) when the electron energy slightly surpasses (by about 0.5-1 eV) the threshold for the production of doubly-charged ions from atoms in the process



These results would provide a sufficient basis for the conclusion that A^{2+} ions result from the autoionization

of A^+ ions if the initial A^+ ions did not possess additional highly-excited states that converge to the first ionization limit and are therefore unable to autoionize although their excitation energies are close to autoionizing states. However, the foregoing discussion points to the existence of such states, which sometimes behave like autoionizing states. For example, the ionization processes of these highly excited states when ions in an electric field collide with residual gas molecules (forming a background), or occurring near the metallic surfaces of collimating slits, are also directly proportional to the intensity of the initial A^+ ions. Nonuniformity of the electron beam energy and a large difference (by a factor of about 10^7) between the intensities of the A^+ ions and the A^{2+} ions produced therefrom according to (1) make it difficult to determine the exact small difference between their thresholds.

In^[9] the ion beams passed through narrow slits. It was therefore possible that a considerable fraction of the A^{2+} ions, which were attributed only to autoionization of A^+ , had resulted from the ionization of highly excited A^{*} ions; these could include ions in autoionizing states, near the metallic surfaces of the slits.

It is therefore necessary to study long-lived autoionizing states of ions under more determinate experimental conditions. Moreover, if singly-charged noble-gas ions should appear in such states, the same should also apply to the corresponding atoms. The present work is an investigation of these effects.

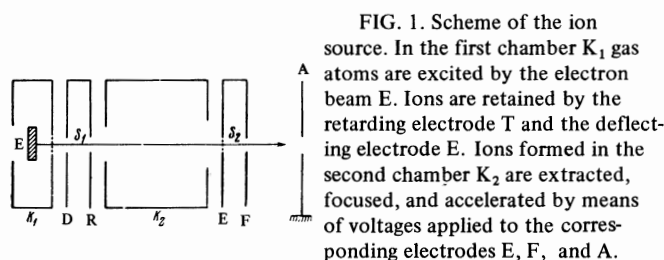
EXPERIMENT

In the mass-spectrometric investigation of long-lived autoionizing states our basic task is the discrimination of these states from lower-lying long-lived highly excited states. The task is difficult because the two types of states have very close energies and, as already mentioned, in some experiments they behave alike. Our work was done with a mass spectrometer and a specially designed ion source that enabled us to discriminate these two kinds of states.

A. Autoionizing States of the Atoms

Figure 1 represents the scheme of the source used

¹⁾We shall here consider only the lowest ionization limits, which are formed by the removal of an outer np^6 electron from an atom or an outer np^5 electron from an ion.



to investigate long-lived excited states of the atoms. The two-chamber ion source that was used in [5] had been changed in the following way. The second chamber K_2 was lengthened to 13 mm in order to permit a larger number of decays; its entrance and exit slits were enlarged to 4×16 and 6×16 mm, respectively, so that the atom beam collimated by the slit $S_1 = 1 \times 8$ mm would not come into contact with the edges of the chamber slits. The narrow slit $S_2 = 1 \times 9$ mm behind the second chamber was covered with a $\sim 70\%$ transparent fine copper grid. This was followed by the exit slit of the ion source. The ions were retained in the first chamber by the retarding field $V_R = 50$ V, the field $V_C = 50$ V of the deflecting condenser, and a ~ 250 -gauss magnetic field that also collimated the electron beam.

A 3.05-kV accelerating potential was applied between the slit S_1 and the electrode A; the potential at the second chamber was 2.8 kV, and that at the slit S_2 with the grid was 2.5 kV. These quantities could be regulated in order to study the influence of the electric fields on the ionization of the highly-excited atoms. The gas pressure in the source region was usually $\sim 10^{-5}$ – 10^{-4} Torr. The ion current was registered with a U1-2 electrometric amplifier.

Figure 2 shows a section of the mass spectrum in the mass-40 region when argon ions are admitted into the source. We see that there are three peaks: peaks 1 and 3 are caused by the Ar^+ ions produced respectively upon ionization of the highly excited Ar^* atoms on the slit S_1 and the grid S_2 , while peak 2 belongs to the ions obtained in the second chamber. They can be produced as a result of the autoionization of the highly-excited argon atoms and when these atoms collide with the unexcited atoms. We can see that the peaks are not symmetrical. This is due mainly to the ionization of the highly-excited atoms in the electric fields in the interelectrode space. When these fields are decreased, the peaks become more symmetrical. An increase of the electric field in the space between K_2 and S_2 leads to a splitting of the second peak.

Figure 3 shows plots of the intensities of all three peaks as functions of the argon pressure. It can be seen that the intensities of all peaks vary linearly with the pressure in the region of low pressures. The nonlinear dependences at high pressures result from collisions in which ions and excited atoms are scattered. The linear dependence of the second peak on Ar pressure provides an argument for its formation by the autoionization of excited Ar^* . The very slight pressure dependence found for the intensity ratio of peaks 2 and 3 (curve 4 in Fig. 3) indicates that the second peak receives only a small contribution from ionization that occurs when excited Ar^* atoms collide with unexcited argon atoms.

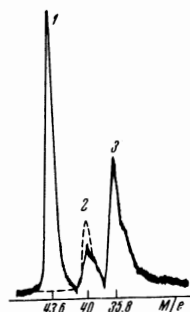


FIG. 2

FIG. 2. A portion of the argon mass spectrum. The dashed peak resulted from reversal of the potential applied between S_1 and K_2 .

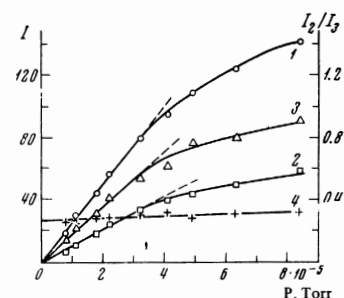


FIG. 3

FIG. 3. Intensities I of Ar^+ ion peaks versus argon pressure. 1, 2, 3—intensities of peaks 1, 2, 3 in Fig. 2; 4—intensity ratio of peaks 2 and 3. For curve 2 the scale of the ordinate axis has been doubled.

Experiments were performed with a reversal of the potential between S_1 and K_2 . The dashed curve in Fig. 2 shows that in this case peak 1 was completely absent. This result was to be expected, because Ar^+ ions from the ionization of highly excited Ar^* at S_1 were retarded and could not enter chamber K_2 . Only peaks 2 and 3 remained.

Completely analogous results were obtained with krypton and xenon; with He the results were entirely different, except in the experiments with reversed polarity. Helium possesses no autoionizing states that lie a little above the ionization threshold, as in the cases of the other noble gases. However, helium does resemble the other atoms in possessing highly excited states lying a little below the ionization threshold.^[4, 5] Therefore helium was a good object for the performance of comparative measurements.

When helium was admitted to the source three peaks were again observed in the vicinity of mass 4. As in Fig. 2, at low pressures the intensities of peaks 1 and 3 were directly proportional to the pressure; this was the result that had been observed for argon, krypton, and xenon. However, the intensity of the middle peak 2, which represents ions from chamber K_2 , is quadratically dependent on pressure in this case. The origin of the peak thus appears to lie in the collisions between highly excited helium atoms and unexcited atoms.

When deuterium is added to the helium peak 2 is augmented by D_2^+ ions produced in the ionization process studied by Penning:



We here find additional confirmation that peak 2 is produced in chamber K_2 .

A similar picture results when helium is added to argon, krypton, or xenon. In these instances the middle peak, representing Ar^+ , Kr^+ , or Xe^+ , is also augmented by the ionization process (3).

The dependence of the peaks on electron energy was also investigated. Here the results were less decisive, for the following reasons. 1) Highly excited autoionizing states, like highly excited non-autoionizing states, are ionized in an electric field near metallic surfaces and in collisions between gas molecules and atoms; there-

fore they can contribute to all peaks. 2) The excitation thresholds of autoionizing states lie very close to the excitation thresholds of the lower-lying non-autoionizing states. 3) Autoionization produces very small ion peaks.

The foregoing circumstances complicate the task of determining differences between the excitation thresholds of the two groups of states and of observing the

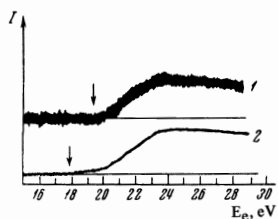


FIG. 4. Excitation curves of xenon. The electron energy scale E_e was not calibrated. 1— Xe^+ ions produced in chamber K_2 , 2— Xe^+ ions produced at slit S_1 . The arrows point to the excitation thresholds of autoionizing and highly excited states.

differences between their excitation functions. For argon and krypton the experimental differences between the thresholds were found to lie within the experimental error limits ± 0.5 eV. Only in the case of xenon do we find, as is shown in Fig. 4, that Xe^{**} atoms in autoionizing states appear at an electron energy that is about 1.5 eV above the production threshold of highly excited Xe^* . The corresponding excitation curve descends somewhat more rapidly as the electron energy is increased. For a detailed investigation of the excitation functions and thresholds we clearly require a good monoenergetic electron beam ($\Delta E < 0.1$ eV) and highly sensitive registering equipment.

B. Autoionizing States of the Ions

We investigated only singly-charged argon ions, which are the most suitable for the present purpose. Long-lived autoionizing states were observed with a mass spectrometer and a special ion source which is sketched in Fig. 5.

Our source enabled us to distinguish between doubly-charged Ar^{2+} ions resulting from the autoionization of Ar^{+*} and other Ar^{2+} ions resulting from different processes, such as ionization at the edges of the collimating slits or ionization in collisions with Ar and background atoms. The source functioned as follows. Ar^+ ions accelerated to 2.8 keV entered chamber K_2 , to which a certain potential $\pm V_K$ was applied. The doubly-charged ions formed in this chamber from singly-charged ions received the following energy: $2.8 \mp V_K$ (the energy of the singly-charged ions entering the chamber) plus $\pm 2V_K$ (received by doubly-charged ions leaving the chamber); the total was $2.8 \pm V_K$. The peak representing these ions could therefore be shifted along the mass scale to a position that is free of overlapping peaks. This peak could be formed by Ar^{2+} ions produced from Ar^{+*} ions by only two processes—autoionization and stripping when argon atoms collide with residual gas molecules.

Ionization of highly excited Ar^{+*} at the edges of the chamber slits was excluded because these slits were very much wider (23×23 mm) than the nearby collimating slits S_1 (1×7 mm) and S_2 (10×10 mm). The dimensions of the remaining slits were 1×4 mm. Chamber K_2 was 210 mm long, and was preceded by a

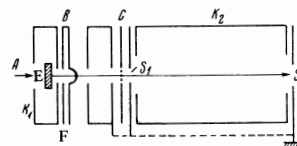


FIG. 5

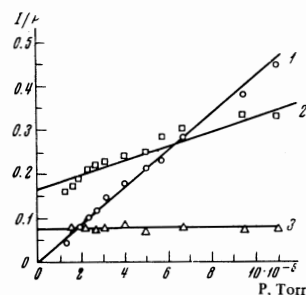


FIG. 6

FIG. 5. Scheme of the ion source. In the first chamber K_1 highly excited ions are produced by collisions between electrons (E) and atoms (A). These ions are extracted (B), focused (F) and directed into the second chamber K_2 , where autoionization occurs. The dashed line connects grounded electrodes.

FIG. 6. Relative ion intensities (in arbitrary units) vs. argon pressure. 1— Ar^+ ions from charge exchange, $\text{Ar}^+ + \text{Ar} \rightarrow \text{Ar} + \text{Ar}^+$; 2— Ar^{2+} ions from chamber K_2 ; 3— Ar^{2+} ions formed at the grid.

grid C at a specified potential. Ar^{+*} ions that passed through the grid lost an electron and were thus converted into Ar^{2+} ions that were registered on the mass scale in accordance with the potential applied to the grid.

The described apparatus was used to study how the intensities of Ar^+ produced in chamber K_2 by collisions of electrons with argon atoms, and of Ar^{2+} produced from singly-charged ions traversing the collimating slits, grid, and chamber K_2 , were influenced by the following factors: Ar pressure, the background, and the electron current and energy. The background pressure was varied by closing valves to reduce the rate of evacuation. The pressure effect of air admitted into the chamber was also studied. Some results are shown in Fig. 6, where we observe that the straight line 2 does not extrapolate to zero with decreasing pressure, which would indicate the absence of autoionization, but intersects the ordinate axis to represent Ar^{2+} ions produced by the autoionization of singly-charged argon ions and by ionizing collisions with residual gas molecules of the mass spectrometer. (Line 1 passes through the origin.) By studying how the pressure of the background and of air admitted to the mass spectrometer influence the intensities of singly- and doubly-charged Ar ions we are enabled to distinguish the foregoing two processes. At the background pressure $\sim 1.5 \times 10^{-7}$ Torr the stripping of singly-charged ions contributes little to the intensity of Ar^{2+} from Ar^{+*} . Therefore most of the Ar^{2+} ions are produced in chamber K_2 by the autoionization of highly excited singly-charged Ar^{+*} . This result is consistent with the conclusion reported in [9, 10] that when electrons collide with Ar atoms a fraction of the Ar^+ ions are formed in long-lived autoionizing states.

DISCUSSION OF RESULTS

Our results indicate that multielectron atoms and ions of noble gases exist in long-lived autoionizing states having lifetimes $\gtrsim 10^{-6}$ sec and lying close to the corresponding ionization limits. In the case of noble-

gas atoms these states lie between the two ionization limits ${}^2P_{3/2}^0$ and ${}^2P_{1/2}^0$ to which respective Rydberg series converge. These states result from the excitation of only a single atomic electron.

The ground level of doubly-charged noble-gas ions is a triplet; the three sublevels 3P_0 , 3P_1 , and 3P_2 of Ar^{2+} are 43.58, 43.53, and 43.93 eV, respectively.^[11] These ions will therefore possess Rydberg series converging to these three ionization limits. The levels that converge to the lowest limit 3P_2 , are highly excited long-lived states,^[2] which do not autoionize. The levels lying above the first ionization limit will autoionize.

The energy E_n of the Rydberg states is represented by

$$E_n = E_\infty - I_H Z^2 / n^{*2}, \quad (4)$$

where E_∞ is the ionization potential of an atom or ion, I_H is the ionization potential of a hydrogen atom, and Z is the charge of the atomic core whose field acts on the highly excited electron. For highly excited atoms $Z = 1$, while for singly-charged ions $Z = 2$; n^* is the effective principal quantum number of the excited state. The latter is somewhat smaller than the principal quantum number n , but when n is large the difference is unimportant and also decreases rapidly as the electron orbital quantum number l increases. In the cases of present interest we can therefore assume $n^* \approx n$.

If E_∞ in (4) is taken to equal the energy required to produce an ion in the excited state $np^5 {}^2P_{1/2}^0$ this equation will give us the energies of the autoionizing atomic levels that we are considering here. Two spontaneous decay modes are possible for an excited autoionizing state: 1) a nonradiative transition into the continuous spectrum (i.e., autoionization), and 2) a radiative transition to a lower level or the ground state. For an allowed transition of the first kind, induced by interelectronic Coulomb interaction, the transition rate is $\sim 10^{15} - 10^{14} \text{ sec}^{-1}$, while for allowed transitions of the second kind it is $\sim 10^9 \text{ sec}^{-1}$. In the cases of the excited atoms and ions that we registered both transitions must be forbidden, or their probabilities are considerably reduced. This follows directly from the experimental result that autoionization of the excited atoms and ions was observed $\sim 10^{-6} \text{ sec}$ after their formation.

For a radiative transition the mean lifetime τ_n of a highly excited hydrogen-like state is dependent on n : $\tau_n \sim 10^{-9} n^4$.^[12] Therefore with $n > 6$ the lifetime will be sufficiently long to permit observation of the described states in our experimental work.

The situation is different with regard to autoionization, which can result from either Coulomb or magnetic interaction between electrons. In both instances the conservation of parity and of the total angular momentum comprise strict selection rules.^[13] For Coulomb autoionization in the case of LS coupling it is also necessary to conserve the total orbital angular momentum L and the total spin S ($\Delta L = 0$, $\Delta S = 0$). However, these are not strict rules and can be violated as a result of magnetic interactions, which lead to an autoionization rate that is reduced by a factor of about 10^8 , as has been observed in the autoionization of alkali atoms.^[13]

We observe that autoionization induced by magnetic interactions occurs at the required rate $\sim 10^6 \text{ sec}^{-1}$. Therefore in this case we have the problem of finding

electronic configurations that autoionize through magnetic interactions. For the noble-gas states of present interest it is known^[14] that LS coupling breaks down because of strong spin-orbit interactions of atomic core electrons. Then jl , or possibly jj , coupling is the more suitable type. The approximate selection rules for autoionization through Coulomb interaction will here be different, of course, and will be derived by a calculation that is outside the scope of the present article. We note only that the strict selection rules (conservation of total angular momentum and parity) hold true for the other types of coupling also.

The considered states of the discrete spectrum lie above the first ionization limit ${}^2P_{3/2}^0$, and the total angular momentum of their atomic core is $J = 1/2$ (${}^2P_{1/2}^0$). Thus, as a result of autoionization the total angular momentum of the atomic core should undergo a unit change ($1/2 \rightarrow 3/2$). This transition can occur only through Coulomb or magnetic interactions between core electrons and excited outer electrons, but not through interactions between electrons within the core.²⁾

Let us consider the case of autoionization due to a Coulomb interaction:

$$V = \sum_{i \neq j} \frac{1}{r_{ij}}, \quad (5)$$

where the subscript j pertains to the excited outer electron. As the principal quantum number is increased the rate of Coulomb autoionization for highly excited states decreases as n^{-3} .^[15] When we start with the normal rate $\sim 10^{14} \text{ sec}^{-1}$ of Coulomb autoionization, we can hardly expect that the described experiments will reveal states with values of n that are high enough to reach the required autoionization rate $\sim 10^6 \text{ sec}^{-1}$. This could occur for $n \gtrsim 100$, but only a negligible probability exists that such states will be excited; moreover, the states could easily be destroyed by electric fields and collisions in the ion source. According to a provisional calculation, under the given experimental conditions the observed effect could include a contribution from states with $n \lesssim 40$. For these values of n the observed lifetimes can be accounted for by associating autoionization with the quadrupole and higher-order terms in the multipole expansion of (5).

All the foregoing considerations with respect to the autoionization of atoms can be applied to singly-charged ions.

Taking^[2, 4, 5, 9, 10] into account, our investigation therefore shows that when electrons collide with the multielectron atoms of noble gases two groups of long-lived highly excited atoms and ions are formed. The first group of excited states consists of high-lying Rydberg states that converge mainly to the first ionization limit $np^5 {}^2P_{3/2}^0$ of an atom, or $np^4 {}^3P_2$ of a singly-charged ion. These are not autoionizing states. The second group includes autoionizing states that lie between the first and second ionization limits. The first group includes optically allowed and forbidden states with $n \gtrsim 6$ and various values of l . The second group includes optically forbidden states with high n and l .

²⁾We neglect the interaction that induces very small hyperfine splitting in the atomic core.^[13]

We are indebted to O. B. Firsov, S. I. Grishanovaya, V. S. Senashenko, and B. M. Smirnov for discussions.

¹Z. Z. Latypov, S. E. Kupriyanov, and N. N. Tunitskiĭ, *Zh. Eksp. Teor. Fiz.* **46**, 833 (1964) [*Sov. Phys.-JETP* **19**, 570 (1964)].

²S. E. Kupriyanov and Z. Z. Latypov, *Zh. Eksp. Teor. Fiz.* **47**, 52 (1964) [*Sov. Phys.-JETP* **20**, 36 (1965)].

³A. S. Newton, A. F. Sciamanna, and R. Clampitt, *J. Chem. Phys.* **46**, 1779 (1967).

⁴V. Čermak and Z. Herman, *Collect. Czechosl. Chem. Commun.* **29**, 953 (1964).

⁵S. E. Kupriyanov, *Zh. Eksp. Teor. Fiz.* **48**, 467 (1965) [*Sov. Phys.-JETP* **21**, 311 (1965)].

⁶S. E. Kupriyanov, *ZhETF Pis. Red.* **5**, 245 (1967) [*JETP Lett.* **5**, 197 (1965)].

⁷H. Hotop and A. Niehaus, *J. Chem. Phys.* **47**, 2506 (1967).

⁸R. E. Huffman, Y. Tanaka, and J. C. Larrabee, *J. Chem. Phys.* **39**, 902 (1963).

⁹N. R. Daly, *Proc. Phys. Soc. (London)* **85**, 897 (1965).

¹⁰A. S. Newton, A. F. Sciamanna, and R. Clampitt, *J. Chem. Phys.* **47**, 4843 (1967).

¹¹A. P. Striganov and N. S. Sventitskiĭ, *Tablitsy spektral'nykh liniĭ (Tables of Spectral Lines)*, Atomizdat, 1966

¹²H. A. Bethe and E. E. Salpeter, *Quantum Mechanics of One- and Two-Electron Atoms*, Academic Press, New York, 1957 (Russ. transl., Fizmatgiz, 1960).

¹³P. Feldman and R. Novick, *Phys. Rev.* **160**, 143 (1967).

¹⁴M. A. El'yashevich, *Atomnaya i molekulyarnaya spektroskopiya (Atomic and Molecular Spectroscopy)*, Fizmatgiz, 1962.

¹⁵U. Fano and J. W. Cooper, *Phys. Rev.* **137**, A1364 (1965).

Translated by I. Emin

174